Proceedings of The Magnetized Plasma in Galaxy Evolution
Sep. 27th – Oct. 1st 2004, Jagiellonian University, Kraków, Poland
Eds. K.T. Chyży, K. Otmianowska-Mazur, M. Soida and R.-J. Dettmar

Cosmic ray driven dynamo in galactic disks

Michał Hanasz[1], H. Lesch[2], K. Otmianowska-Mazur[3], and G. Kowal[3]

[1]Centre for Astronomy, Nicholas Copernicus University, PL-87148 Piwnice/Toruń, Poland
[2]Astronomical Observatory, Munich University, Scheinerstr. 1, D-81679, Germany
[3]Astronomical Observatory, Jagiellonian University, ul. Orla 171, 30-244 Kraków

Abstract

We present the first numerical model of the magnetohydrodynamical dynamo, driven by cosmic rays in the interstellar medium. The cosmic rays are produced in randomly occurring supernova remnants. Our model is described by equations of magnetohydrodynamics supplemented with the diffusion-advection equation governing the propagation of cosmic rays. The other essential elements of the model are: vertical gravity of the disk, differential rotation and resistivity leading to reconnection of magnetic field lines. We obtain amplification of the large-scale magnetic field on a timescale of galactic rotation. The model represents a kind of fast, cosmic ray driven galactic dynamo proposed by Parker (1992). The amplification of the large-scale magnetic field results from the buoyancy of the cosmic ray component in the interstellar medium.

1 Introduction

The dynamo theory applied to galactic magnetic fields successfully reproduces majority of observational features of large scale galactic magnetic fields (Ruzmaikin et al. 1988, Beck et al. 1996, Vallée 2004). The dynamo process is a combination of differential rotation, helical turbulence and a dissipative process. The exponential growth time of galactic magnetic fields, characteristic for classical mean field dynamos relying on turbulent motions powered by supernova explosions, is typically estimated to be of the order of $t_{\mathrm{dynamo}} \sim (5-10) \times 10^8$ yr. Despite successes of the dynamo theory, serious criticism against it has been raised by Kulsrud & Anderson (1992) and Vainshtein & Cattaneo (1992). These authors conclude that the cascade of magnetic energy toward diffusive scales is blocked by the Lorentz force and turbulent diffusivity as well as the α-effect are catastrophically reduced (see the review by Widrow (2002) and references therein).

An attractive idea of a *fast galactic dynamo* offering a solution of the classical dynamo problems has been proposed by Parker (1992). The idea relies on two new fundamental ingredients: (1) cosmic rays (CR) continuously supplied to the disk by supernova (SN) remnants and (2) fast magnetic reconnection which operates in current sheets and makes it possible to dissipate and relax the random magnetic field component even in the limit of vanishing resistivity. Over the last decade we have investigated the different physical properties and consequences of Parker's idea and scenario by means of analytical calculations and numerical simulations (Hanasz & Lesch 1993, 1997, 1998, 2000, 2001, 2003a,b ; Hanasz et al. 2002, Lesch & Hanasz 2003, Kowal et al. 2003). Here we review the first complete magnetohydrodynamical three-dimensional simulations including the full network of relevant interacting mechanisms.

The dynamo amplification of galactic magnetic fields is attributed to properties of a complex, multicomponent interstellar medium (ISM). It follows from observational data (see eg.

Beck et al. 1996, Beck 2004 and references therein) that all the three components appear in approximate energetic equipartition i.e. $U_{\rm gas} \simeq U_{\rm mag} \simeq U_{\rm CR} \sim 1{\rm eV}/\,{\rm cm}^3$. This indicates that they are dynamically coupled, i.e. an energy excess of each component can be converted into energy of other two components.

The major source of ISM disturbances are the SN type II explosions (Mac Low & Klessen 2004), whose kinetic energy supply to the ISM is of the order of $\sim 10^{51}$ erg/SN. This energy is distributed into three channels: 10 div 50 % is spent for accelleration of cosmic rays (e.g. Jones et al. 1998), 40 div 80 % for heating of the ISM and the remaining 10 % for kinetic energy of turbulence.

The cosmic ray (CR) component of ISM gas, consists of relativistic electrons, protons and heavier atomic nuclei (see eg. Berezinski et al. 1990). The cosmic ray particles are accelerated in supernova remnants (SNR) within galactic disks (Koyama et al. 1995). Although the velocity of individual CR particles is close to the speed of light, the bulk motion of CR is diffusive and the CR bulk speed is of the order of Alfvén speed (Kulsrud & Pearce 1969), i.e. typically a few tens of km/s. Recent studies by Giacalone and Jokipii (1998) and Jokipii (1999) suggest that the diffusion of cosmic ray gas in a turbulent magnetic field proceeds preferentially along the direction of the mean magnetic field.

2 Description of the cosmic ray transport

The diffusive cosmic ray transport in galactic disks can be described by the diffusion-advection equation. Following Schlickeiser and Lerche (1985) we apply the following form of the transport equation

$$\frac{\partial e_{\rm cr}}{\partial t} + \boldsymbol{\nabla}(e_{\rm cr}\boldsymbol{V}) = -p_{\rm cr}\boldsymbol{\nabla}\boldsymbol{V} + \boldsymbol{\nabla}(\hat{K}\boldsymbol{\nabla}e_{\rm cr}) + Q_{\rm cr} \tag{1}$$

$$p_{\rm cr} = (\gamma_{\rm cr} - 1)e_{\rm cr} \tag{2}$$

where $e_{\rm cr}$ and $p_{\rm cr}$ are CR energy density and pressure, $\gamma_{\rm cr}$ is the CR specific heat ratio (we assume $\gamma_{\rm cr} = 14/9$ following the argumentation by Ryu et al. 2003), $\boldsymbol{V}$ is the thermal gas velocity, $\hat{K}$ is the CR diffusion tensor and $Q_{\rm cr}$ represents CR source term representing the CR output from supernova remnants.

The anisotropic diffusion of cosmic rays can be implemented through the following form of the diffusion tensor (see eg. Ryu et al. 2003)

$$K_{ij} = K_{\perp}\delta_{ij} + (K_{\parallel} - K_{\perp})n_i n_j, \quad n_i = B_i/B, \tag{3}$$

where, following Giaccalone and Jokipii (1998), we assume that $K_{\perp}/K_{\parallel} \sim 0.05$ for $\boldsymbol{B}_{\rm turb} \sim \boldsymbol{B}_{\rm uniform}$.

The diffusion-advection equation (1) tells us how the cosmic ray component propagation is influenced by the dynamics of a magnetized medium. One should note however that that the cosmic ray component itself contributes to the dynamics of the thermal gas. This is because every scattering event of cosmic ray particles, against magnetic fluctuations, transfers energy and momentum to the gas component. Therefore an additional source term: $-\nabla p_{\rm CR}$ is necessary on the r.h.s. of the equation of gas motion (see eg. Berezinski et al. 1990).

In order to study the dynamics of magnetized ISM including cosmic rays and the cosmic ray driven dynamo we added the cosmic ray component described by the diffusion-advection

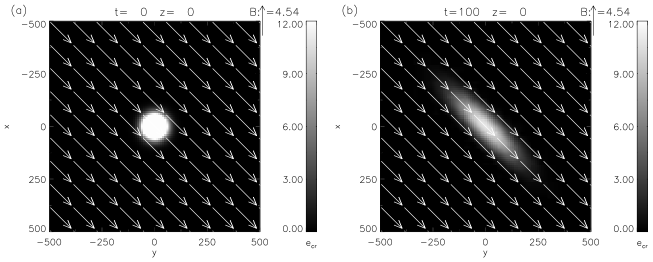

Figure 1: Passive CR transport. (a) initial CR energy density distribution and magnetic field vectors, (b) same after several diffusion times ($t = 100$), where one can note only the effect of CR-diffusion.

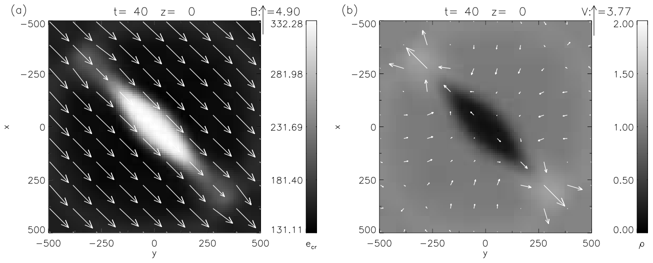

Figure 2: Active CR transport. (a) CR energy density distribution and magnetic field at $t = 40$, (b) gas density and velocity vectors. The cavity in thermal gas distribution, two regions of compressed gas and the apparent gas flow are due to the action of cosmic rays.

equation (1) into the Zeus-3D MHD code (Stone & Norman 1992a,b). The numerical algorithm has been described by Hanasz & Lesch (2003b). Our modifications of the Zeus-3D code include also incorporation of the explicit resistivity in the induction equation (Hanasz et al 2002), vertical disk gravity following the model of ISM in the Milky Way by Ferriere (1998), shearing-periodic boundary conditions and rotational pseudoforces (Hawley, Gammie and Balbus 1995).

3 Examples of dynamical effects of cosmic rays

In order to illustrate qualitatively the diffusive transport of cosmic rays we inject a portion of cosmic rays locally, in the mid of the computational box permeated by a diagonal magnetic field. First we consider a case of passive cosmic ray transport by neglecting the term $-\nabla p_{\rm CR}$ in the equation of gas motion. The passive cosmic ray diffusion along the direction of magnetic field is shown in Fig. 1. The next example presented in Fig. 2 shows the dynamical role of cosmic rays when the term $-\nabla p_{\rm CR}$ is included in the equation of gas motion. The additional pressure of cosmic rays pushes the gas along with the frozen-in magnetic field lines away from the cosmic ray injection region. The thermal gas, primarily accelerated along the magnetic field lines, starts to form two regions of enlarged density on both sides of the ellipsoidal cavity.

Another numerical experiment demonstrates the effect of local cosmic ray injection on the vertically stratified disk equilibrium (see Hanasz & Lesch 2003b). In Fig. 3 we show the

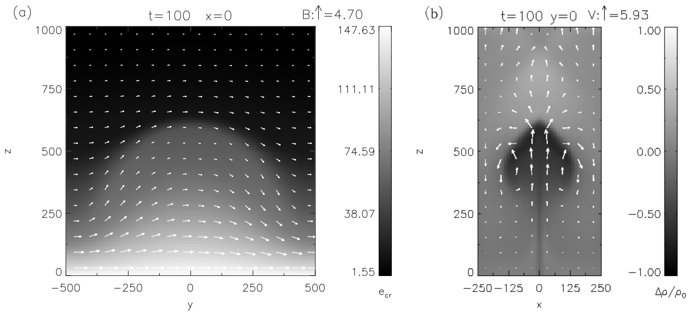

Figure 3: Parker loop formed due to cosmic rays produced in a supernova remnant in a vertically stratified atmosphere. (a) cosmic ray energy density and magnetic vectors in the vertical plane parallel to the initial magnetic field direction, (b) thermal gas density and velocity vectors in the plane perpendicular to the flux tube. A buoyant motion of an underdense fluxtube is apparent.

evolution of a magnetic flux tube which has been enriched with cosmic ray gas by a supernova explosion. Due to the contribution of CR pressure in the total pressure the flux tube inflates locally and then becomes lighter than the surrounding medium (see Fig. 3 (b)). In presence of vertical gravity it starts to rise as a result of its buoyancy. The Parker loop apparent in Fig. 3 (a) is formed on a timescale of 100 Myr.

4 Numerical simulations of the CR-driven dynamo

The first complete 3D numerical model of the CR-driven dynamo has been demonstrated by Hanasz et al. (2004). The presented numerical simulations were performed with the Zeus-3D MHD code extended with: the cosmic rays supplied by supernova remnants randomly exploding in the disk volume, resistivity of the ISM leading to magnetic reconnection, shearing-periodic boundary conditions, rotational pseudo-forces and a realistic vertical disk gravity.

We performed numerical simulations in a 3D Cartesian domain $500\,\mathrm{pc} \times 1000\,\mathrm{pc} \times 1200\,\mathrm{pc}$, extending symmetrically around the galactic midplane from $z = -600\,\mathrm{pc}$ up to $z = 600\,\mathrm{pc}$, with the resolution of $50 \times 100 \times 120$ grid zones in directions x, y and z, corresponding locally to cylindrical coordinates r, ϕ and z, respectively. The applied boundary conditions are periodic in the y-direction, sheared-periodic in the x direction and outflow in the z direction. The assumed disk rotation is represented locally by the angular velocity $\Omega = 0.05\,\mathrm{Myr}^{-1}$ and by a flat rotation curve. We apply the vertical gravity profile determined for the Solar neighborhood. We assume that supernovae explode with the frequency $2\mathrm{kpc}^{-2}\,\mathrm{Myr}^{-1}$ (which is about 10 % of the value estimated for the Solar neighborhood), and assume that 10 % of the 10^{51}erg kinetic energy output from SN is converted into the CR energy. The CR energy is injected instantaneously into the ISM with a Gaussian radial profile ($r_{SN} = 50\mathrm{pc}$) around the explosion center. The explosion centers are located randomly with a uniform distribution in the x and y directions and with a Gaussian distribution (scaleheight $H = 100\mathrm{pc}$) in the vertical direction. The applied value of the CR parallel diffusion coefficient is $K_\parallel = 10^4\mathrm{pc}^2\mathrm{Myr}^{-1} = 3 \times 10^{27}\,\mathrm{cm}^2\,\mathrm{s}^{-1}$ (i.e. 10 % of the realistic value) and the perpendicular

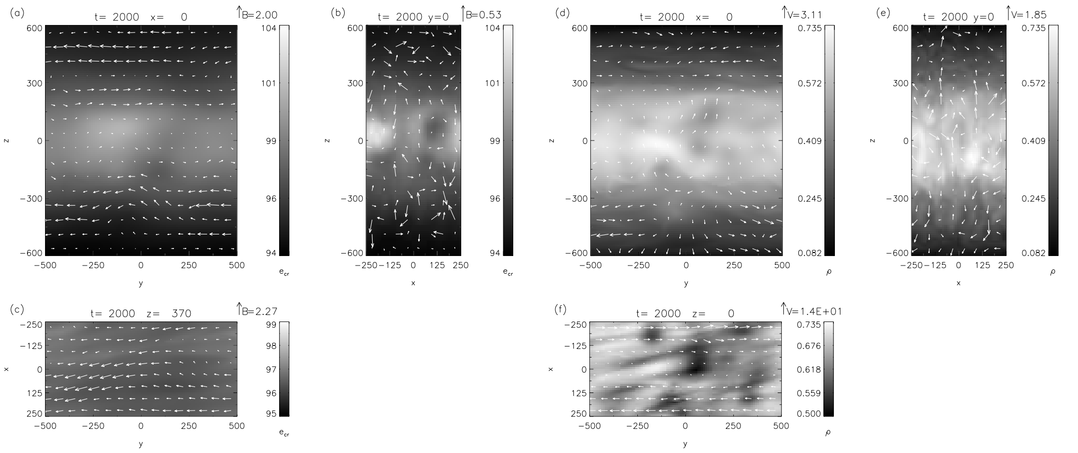

Figure 4: Slices through the computational volume at $t = 2000\,\mathrm{Myr}$. Panels (a),(b) and (c) show CR energy density with vectors of magnetic field in yz, xz and xy planes respectively, panels (d), (e) and (f) show gas density with velocity vectors in the same planes.

one is $K_\perp = 10^3\,\mathrm{pc}^2\,\mathrm{Myr}^{-1} = 3 \times 10^{26}\mathrm{cm}^2\mathrm{s}^{-1}$. The applied resistivity is $\eta = 1\,\mathrm{pc}^2\,\mathrm{Myr}^{-1} = 3 \times 10^{23}\,\mathrm{cm}^2\,\mathrm{s}^{-1}$. The initial state of the system is a magnetohydrostatic equilibrium with a horizontal purely azimuthal magnetic field corresponding to $p_{\mathrm{mag}}/p_{\mathrm{gas}} = 10^{-8}$. The initial CR pressure in the initial state is equal to zero. The initial gas density at the galactic midplane is 3 H atoms cm^{-3} and the initial isothermal sound speed is $c_{\mathrm{si}} = 7\,\mathrm{km\,s}^{-1}$.

5 Simulation results

Fig. 4 shows the distribution of CR gas together with magnetic field, and thermal gas density together with gas velocity in the computational volume at $t = 2000$ Myr. In panel (a) we notice a dominating horizontal alignment of magnetic vectors, which is persistent over the whole simulation time. The CR energy density is well smoothed by the diffusive transport in the computational volume. The vertical gradient of the CR energy density is maintained by the supply of CRs around the equatorial plane in the disk in the presence of vertical gravity. In panel (c) one can notice that the dominating magnetic vectors at the height $z = 370\,\mathrm{pc}$ are inclined with respect to the azimuthal direction, i.e. the radial magnetic field component is on average about 10 % of the azimuthal one. The CR energy density is displayed in scaled units.

6 Amplification and structure of the mean magnetic field

In the following Fig. 5 we show how efficient is the amplification of mean magnetic field resulting from the continuous supply of CRs in supernova remnants. First we note the growth of the total magnetic energy, by 7 orders of magnitudes during the period of 2 Gyr. Starting from $t \sim 300$ Myr the growth of magnetic energy represents a straight line on a logarithmic plot, which means that the magnetic energy grows exponentially. The e-folding time of magnetic energy determined for the period $t = 400\,\mathrm{div}\,1500$ Myr is 115 Myr. Around $t = 1500$

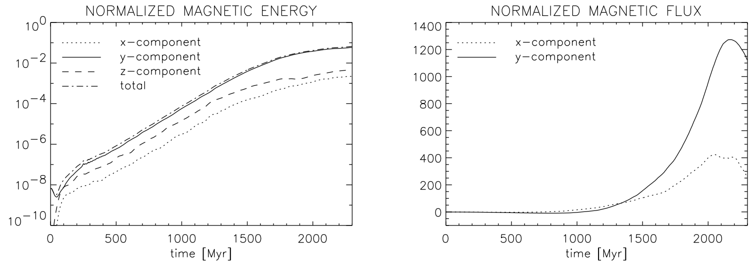

Figure 5: Evolution of magnetic field in the computational volume. The left panel shows the total magnetic energy normalized to the initial gas thermal energy (dash-dot line) along with normalized energies of azimuthal magnetic field (full line), radial magnetic field (dotted line) and vertical magnetic field (dashed line). The right panel shows the evolution of azimuthal magnetic flux $\times(-1)$ (full line) and radial magnetic flux $\times 10$ (dotted line), both normalized to the initial value of the azimuthal magnetic flux.

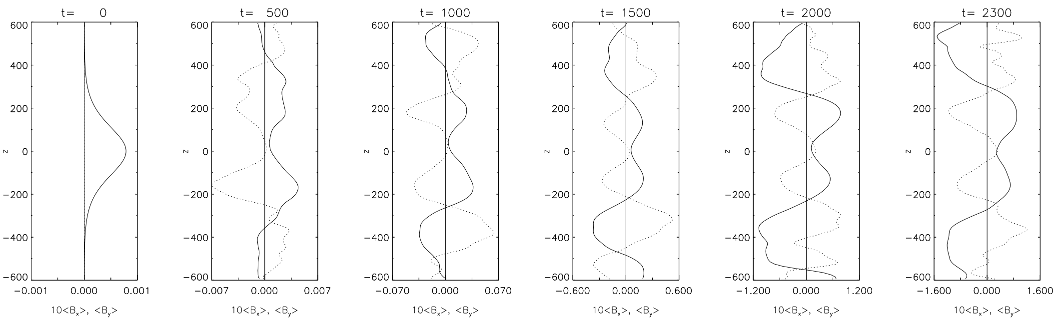

Figure 6: Vertical structure of the mean magnetic field for a sequence of time instants. Spatial averaging is done over planes z=const. Full line represents the mean azimuthal magnetic field and dotted line the radial magnetic field multiplied by 10. The amplification effect is reflected in the varying range of the horizontal axis.

Myr, the growth starts to slow down as the magnetic energy approaches an equipartition with the gas energy.

The other three curves in the left panel of Fig. 5 show the growth of energy of each magnetic field component. It is apparent that the energy of radial magnetic field component is almost an order of magnitude smaller than the energy of vertical magnetic field component which is almost one order of magnitude smaller than the energy of the azimuthal one. This indicates that the dynamics of the system is dominated by the buoyancy of CRs and that magnetic reconnection efficiently cancels the excess of the random magnetic fields.

In the right panel of Fig. 5 we show the time evolution of the normalized, mean magnetic fluxes $\Phi_x(t)/\Phi_y(t=0)$ and $\Phi_y(t)/\Phi_y(t=0)$, where $\Phi_x(t)$ and $\Phi_y(t)$ are respectively magnetic fluxes at moment t, threading vertical planes perpendicular to x and y axes respectively, and averaging is done over all possible planes of a given type. We find that the radial magnetic flux Φ_x starts to deviate from zero, as a result of Coriolis force and open boundary conditions.

Due to the presence of differential rotation the azimuthal magnetic field is generated from the radial one. The azimuthal flux grows up by a factor of 10 in the first 800 Myr of the system evolution and then drops suddenly, reverts and continues to grow with the opposite sign undergoing amplification by more three orders of magnitudes, with respect to the initial value.

In order to examine the structure of the mean magnetic field we average B_x and B_y across constant z-planes. The results are presented in Fig. 6 for $t = 0$ (the initial magnetic field) and then for $t = 500$, 1000, 1500, 2000 and 2300 Myr. We find that the mean magnetic field grows by a factor of 10 within about 500 Myr, which gives an e-folding time close to 250 Myr. We note that an apparent wavelike vertical structures in $\langle B_x \rangle$ and $\langle B_y \rangle$ are formed from the initial purely azimuthal, unidirectional state of B_y and $B_x = 0$. The evolved mean magnetic field configuration reaches a quasisteady pattern which grows in magnitude with apparent vertical reversals of both components of the mean magnetic field. We note also that the magnetic field at the disk midplane remains relatively weak.

A striking property of the mean magnetic field configuration is the almost ideal coincidence of peaks of the oppositely directed radial and azimuthal field components. This property corresponds to a canonical picture of the $\alpha - \Omega$-dynamo: the azimuthal mean magnetic component is generated from the radial one and vice versa.

It is worthwhile to make a comment on the role of the major parameters of the system on the efficiency of the CR-driven dynamo process. On the base of the other (unpublished) numerical experiments we note that increasing the SN frequency and the CR diffusion coefficients leads to shorter timescales of amplification of the large-scale magnetic fields. If for instance $f_{\rm SN} = 5 {\rm kpc}^{-2}\,{\rm Myr}^{-1}$, $K_\parallel = 3 \times 10^{28}\,{\rm cm}^2\,{\rm s}^{-1}$, $K_\perp = 3 \times 10^{27}\,{\rm cm}^2\,{\rm s}^{-1}$ then the amplification timescale of the mean magnetic field drops down to about 180 Myr.

If, on the other hand, the explicit resistivity is reduced to zero then we note a qualitative change of the nature of the amplification process. This can be noted by comparing the magnetic energy evolution and spectra of magnetic fluctuations for the above discussed simulation with $\eta = 1\,{\rm pc}^2\,{\rm Myr}^{-1}$ against a corresponding ideal case ($\eta = 0$).

In the ideal case ($\eta = 0$) we find that the magnetic field energy starts to grow more rapidly around $t = 250$Myr, i.e. it grows by 4 orders of magnitude in subsequent 100 Myr which corresponds to the e-folding time of the magnetic field strength $t_{\rm MF} = 22$Myr. Such a growthtime of magnetic field appears very close to the expected growthtime of the most unstable mode of magnetorotational instability, which is $t_{\rm BH} = 1/\Omega = 1/(0.05{\rm Myr}^{-1}) =$ 20Myr.

On the other hand we note that the evolution of the spatial spectrum of fluctuations of B_x along the z direction differs in the ideal case with respect to the resistive one. In the resistive case the spectrum is flat in the small wavenumber limit and is close to the powerlow with the index $p = -5/3$ for large wavenumbers during the simulation time. In the ideal case small-scale fluctuations start to develop after $t = 250$ and become dominating around $t = 300$Myr. The appearance of the short-wavelength magnetic fluctuations after $t = 250$Myr can be explained by the onset of the magnetorotational instability. Magnetic field is so weak at the beginning of our simulations ($B \sim 10^{-9}$G) that the wavelength of the most unstable modes is much smaller than the cell size in numerical simulations. Due to the initial dynamo amplification magnetic field becomes sufficiently strong for excitation of the large-k modes of the magnetorotational instability after $t = 250$Myr. These short wavelength modes appear in the magnetic fluctuation spectrum. The magnetorotational instability itself is capable of amplifying magnetic field (see Dziourkevich et al. this volume) thus we observe the growth of magnetic energy on the timescale $t_{\rm MF} = 22$Myr. The magnetic energy is, in the discussed ideal case, cumulated in the small-scale component inducing formation of numerous current sheets. In the presence of explicit resistivity these current sheets are sites of magnetic reconnection which damps out the very short wavelengths modes of the magnetorotational instability. Therefore, the observed magnetic field amplification in the presented resistive MHD simulations with cosmic rays should be attributed to the buoyancy of cosmic rays rather than to the magnetorotational instability.

7 Summary and conclusions

We have performed the first numerical experiment in which amplification of the large-scale magnetic field appeared as a solution of the system of resistive MHD equations along with the CR diffusive transport equation. The experiment has shown that the supply of cosmic rays into the ISM by randomly distributed supernova remnants leads to the buoyancy phenomenon and then to the generation of both radial and azimuthal magnetic fields in presence of Coriolis force and differential rotation.

The amplification of the large scale magnetic field proceeds on a timescale ≤ 250 Myr, showing a tendency to decrease for larger (and more realistic) supernova rates as well as larger (and more realistic) CR diffusion coefficients. The overall amplification of the large scale magnetic induction by almost 4 orders of magnitude took about 2 Gyr. The pitch angles of the large scale magnetic fields generated in our experiments range from 10^o to 20^o.

The general conclusion from the presented work is that the cosmic-ray driven dynamo proposed by Parker's (1992) works very efficiently and is capable of amplifying the galactic magnetic fields by several orders of magnitudes starting from very weak magnetic fields and ending close to the equipartition values.

The short timescale of magnetic field amplification in our experiments implies that large scale magnetic fields ($\geq 1\mu$G) should be expected in very young galaxies at cosmological redshifts $z = 1 \,\mathrm{div}\, 2$. This result is consistent with the observations of μG magnetic fields in early galaxies by Kronberg & Perry (1982) and Wolfe, Lanzetta & Oren (1991).

Acknowledgements

The work on this paper has been supported by the Polish Committee for Scientific Research (KBN) through the grant 1 P03D 004 26 and by the Alexander von Humboldt Foundation.

References

Beck, R. 2004, Ap&SS, 289, 293

Beck, R., Brandenburg,A., Moss, D., Shukurov, A., Sokoloff, D.: 1996, ARA&A 34, 155

Berezinskii, V.S., Bulanov, S.V., Dogiel, V.A., Ginzburg, V.L., Ptuskin, V.S., *Astrophysics of cosmic rays*, Amsterdam: North-Holland, 1990.

Ferriere, K., 1998, ApJ, 497, 759

Giaccalone & Jokipii, 1998, ApJ, 520, 2004

Hanasz, M., Lesch, H., 1993, A&A, 278, 561

Hanasz, M., Lesch, H., 1997, A&A, 321, 1007

Hanasz, M., Lesch, H., 1998, A&A, 332, 77

Hanasz, M. Lesch, H., 2000, ApJ, 543, 235

Hanasz, M. Lesch, H., 2001, Space Sci. Rev., 99, 231.

Hanasz, M., Otmianowska-Mazur, K., Lesch, H., 2002, A&A, 386, 347

Hanasz, M., Lesch, H., 2003a, A&A, 404, 389

Hanasz, M., Lesch, H., 2003b, A&A, 412, 331

Hanasz, M., Kowal, G., Otmianowska-Mazur, K., & Lesch, H., 2004, ApJ 605, L33

Hawley, J.F., Gammie, C.F., Balbus, S.A., 1995, ApJ, 440, 442

Jones, T.W., Rudnick, L., Jun, B.-I. et al., 1998, PASP 110, 125

Jokipii, J.R., 1999, *in* J. Franco and A. Carraminana (eds.) *Interstellar Turbulence*, Cambridge University Press, p. 70.

Kowal, G., Hanasz, M., Otmianowska-Mazur, K., 2003, A&A, 404, 533

Koyama, K.P., Petre, P., Gotthelf, E.V., et al., 1995, Nature, 378, 255

Kronberg, P.P., Perry, J.J., 1982, ApJ, 263, 518

Kulsrud, R.M., Anderson, S.W., 1992, ApJ, 396, 606

Kulsrud, R., Pearce, S., 1969, ApJ, 156, 445

Lesch, H., Hanasz, M., 2003, A&A, 401, 809

Mac Low, M.M, Klessen, R., 2004, RvMP 76, 125

Schlickeiser, R., Lerche, I., 1985, A&A, 151, 151

Stone, J.M., Norman, M.L, 1992a, ApJS, 80, 753

Stone, J.M., Norman, M.L, 1992b, ApJS, 80, 791

Parker, E.N., 1992, ApJ, 401, 137

Ruzmaikin, A.A., Shukurov, A.M., Sokoloff, D.D., 1988, *Magnetic Fields of Galaxies* (Dordrecht: Kluwer)

Ryu, D., Kim, J., Hong, S.S., Jones, T.W., 2003, Apj, 589, 338

Vainshtein, S.I., Cattaneo, F., 1992, ApJ, 393, 165

Vallée, J.P., 2004, NewAR, 48, 763

Widrow, L., 2002, RvMP, 74, 775

Wolfe, A.M., Lanzetta, K.M., Oren, A.L., 1992, ApJ, 388, 17